

# Numerical Investigation of Externally Venting Flame Characteristics in a Corridor-Façade Configuration

Asimakopoulou E.<sup>1,\*</sup>, Chotzoglou K.<sup>1,2</sup>, Kolaitis D.<sup>3</sup>, Zhang J.<sup>1</sup>, Delichatsios M.A.<sup>4,5</sup>

<sup>1</sup> FireSERT, School of Architecture and the Built Environment, Ulster University, UK

<sup>2</sup> Efectis, UK/Ireland

<sup>3</sup> Laboratory of Heterogeneous Mixtures and Combustion Systems,  
School of Mechanical Engineering, National Technical University of Athens, Greece

<sup>4</sup> Northeastern University, Boston, USA

<sup>5</sup> University of Science and Technology of China, Hefei, China

\*Corresponding author's email: [e.asimakopoulou@ulster.ac.uk](mailto:e.asimakopoulou@ulster.ac.uk)

## ABSTRACT

Understanding of the physics and mechanisms of fire development and Externally Venting Flames (EVF) in corridor-like enclosures is fundamental to studying fire spread to adjacent floors in high-rise buildings. The main scope of this study is to investigate the burning behaviour of a liquid fuel pool fire in a corridor-like enclosure, to identify the key factors influencing EVF characteristics, EVF impact on façades and to assess the ability of currently available CFD tools to adequately describe corridor-façade fires. The Fire Dynamics Simulator (FDS) CFD tool is used for the numerical simulations which are compared and validated against medium scale experimental data on corridor-façade fire experiments. Experimental results suggest that, in the interior of the corridor, good qualitative and occasionally quantitative agreement is observed for the gas temperatures. When the burner is positioned at the back of the corridor, resulting in increased temperatures at the interior, FDS generally underpredicts the combustion zone and the fire plume seems tilting at the rear of the corridor. The performance of the CFD tool in predicting EVF gas temperatures and heat flux to the adjacent façade is improved in larger opening sizes. Regarding the heat flux at the exposed surface of the façade, good quantitative agreement is observed, especially at lower heights near the opening.

**KEYWORDS:** Corridor-façade fire, externally venting flames, numerical investigation.

## INTRODUCTION

Understanding the characteristics of compartment fire development and externally venting flames (EVF) is fundamental for studying fire spread in high-rise buildings or to adjacent structures. Even though significant effort has been devoted to studying the fire development in cubic-like enclosures, limited data exist for more complex geometries that are most commonly used in modern construction, such as corridor-like enclosures. Studies [1-3] have indicated the need to further progress knowledge related to the understanding of the physics of fire growth in corridor-like enclosures and the mechanisms that eventually may lead to fire spread.

Experimental work by the author's group in fire and burning behaviour in corridor-like enclosures using liquid pool fires, revealed that for most cases three distinct burning regions (*Region I, II and III*) have been observed, corresponding respectively to fuel-controlled, ventilation-controlled and steady-state burning. The duration of each region depends on both the pan size and ventilation factor. *Region I* corresponds to the fuel-controlled period (growth period), where the combustion efficiency is close to unity and thus  $Q_{exp}$ , and  $Q_{th}$ , are almost equal. After this phase, during

Proceedings of the Ninth International Seminar on Fire and Explosion Hazards (ISFEH9), pp. 459-468

Edited by Snegirev A., Liu N.A., Tamanini F., Bradley D., Molkov V., and Chaumeix N.

Published by St. Petersburg Polytechnic University Press

ISBN: 978-5-7422-6496-5 DOI: 10.18720/spbpu/2/k19-39

*Region II*, the fire gradually becomes ventilation-controlled and  $Q_{exp}$  reaches a plateau until the flames eject through the opening. Note that  $Q_{exp}$  inside the enclosure does not reach the maximum value, estimated as  $1500A_oH_o^{1/2}$ , that has been found for rectangular compartments [4]. This value is decreased, calculated to be approximately  $1100A_oH_o^{1/2}$ , indicating that the amount of air inflow in long corridors is less than in rectangular enclosures with the same opening geometry [5]. Flames ejection, as observed visually and through the image processing algorithm, is associated with a sudden increase in the  $Q_{exp}$ , indicating the beginning of *Region III*, where sustained external burning is observed until a plateau is formed near the end of the test indicating that steady-state conditions are established. For the cases when ventilation-controlled conditions are achieved, the normalized steady-state mass burning rate is found to increase linearly with the normalized ventilation factor, which is consistent with previous findings with cubic-like enclosures. The effect of opening size on the air flow rate into the corridor was also examined, and the ventilation coefficient,  $C$ , for corridor-like enclosures during post-flashover conditions was found to decrease with an increase of the ventilation factor. The location and size of the fuel pan was also found to have a strong impact on HRR and subsequent EVF characteristics [3].

Currently, there are no specific methodologies to evaluate risks associated with EVF in “performance-based” fire safety codes and only few numerical simulation studies have been carried out on the burning characteristics of EVF in corridors and relevant façade fire safety issues. To close this knowledge gap, this study is aimed at investigating numerically the burning behaviour of liquid fuel pool fires in corridor-like geometries in order to identify the key factors influencing EVF characteristics and their impact on the façade. The large-eddy-simulation (LES) based CFD code, Fire Dynamics Simulator (FDS) version 6.7.0, was used and the simulation results are compared and validated against experimental data obtained by the authors’ group [1]. The FDS predictive accuracy of the upper layer gas temperatures in enclosures [6, 7, 8] is found to be limited, the main drawback being the insufficient representation of the combustion inefficiencies during under-ventilated fires [6, 8]. Despite the above-mentioned limitations, FDS may adequately be used for a qualitative assessment of the parameters that may influence the medium-scale enclosure fire development [9, 10, 11]. A wealth of information regarding the detailed characteristics of the flow- and thermal-field developing inside or outside the compartment can be provided and as a result, the thermal impact of EVF on the façade elements can be thoroughly assessed. A parametric study has also been performed to further investigate the effects of ventilation and location of the burner.

## RESULTS AND DISCUSSION

### Experimental and numerical set-up

Figure 1 shows a schematic view of the experimental set-up along with the experimental measurement locations, consisting of temperatures inside the corridor, heat fluxes on the floor of the corridor enclosure and on the façade, heat release rate, mass loss rate and flame height of the EVF [1], which was closely reproduced in the numerical setup.

The effect of ventilation was investigated by altering the dimensions of the opening. Four different door-like openings were used, with their dimensions shown in Table 1, and two different load cell positions were investigated. A summary of the main operational parameters, i.e., burner position, opening height ( $H_o$ ), opening width ( $W_o$ ), total fire duration ( $t_{dur}$ ), total heat release rate ( $HRR$ ) experimentally measured in the hood ( $\dot{Q}_{exp}$ ), theoretical  $HRR$  ( $\dot{Q}_{th}$ ) and ventilation regime (Under or Over ventilated, indicated as U or O, respectively).  $\dot{Q}_{th}$  is calculated by multiplying the measured fuel mass loss rate by the heat of combustion of ethanol, 26.78 MJ/kg [12]. The maximum  $HRR$  in stoichiometric conditions inside an enclosure,  $1500A_oH_o^{1/2}$ , is calculated [12].

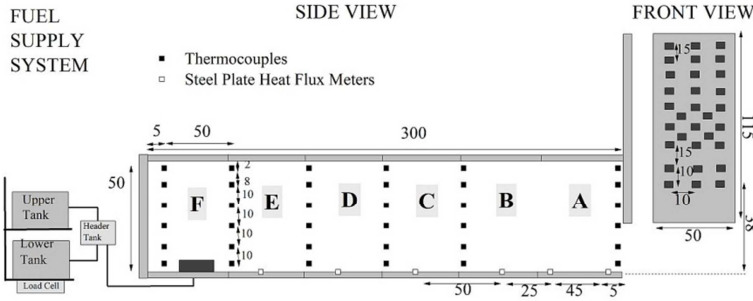


Fig. 1. Schematic of the experimental facility.

Table 1. Summary of main operational parameters for the examined test cases

| Test cases | Burner position | $W_oH_o$ [m <sup>2</sup> ] | $1500A_oH_o^{1/2}$ [kW] | $Q_{exp}$ [kW] | $Q_{th}$ [kW] | Regime | $t_{dur}$ |
|------------|-----------------|----------------------------|-------------------------|----------------|---------------|--------|-----------|
| FR30W25H25 | BOX A           | 0.25 x 0.25                | 46.5                    | 31.0           | 42.7          | O      | 1200      |
| FR30W30H30 |                 | 0.30 x 0.30                | 73.5                    | 56.1           | 75.3          | U      | 1282      |
| FR30W50H25 |                 | 0.50 x 0.25                | 93.8                    | 75.1           | 102.0         | U      | 1869      |
| FR30W50H50 |                 | 0.50 x 0.50                | 265.1                   | 69.5           | 91.1          | O      | 1296      |
| BC30W25H25 | BOX F           | 0.25 x 0.25                | 46.9                    | 39.5           | 64.5          | U      | 1100      |
| BC30W30H30 |                 | 0.30 x 0.30                | 73.9                    | 70.0           | 110.6         | U      | 1128      |
| BC30W50H25 |                 | 0.50 x 0.25                | 93.8                    | 77.0           | 120.5         | U      | 1008      |
| BC30W50H50 |                 | 0.50 x 0.50                | 265.1                   | 105            | 150.0         | O      | 1815      |

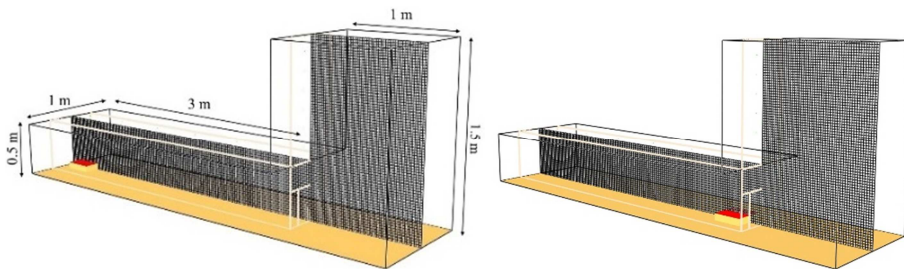
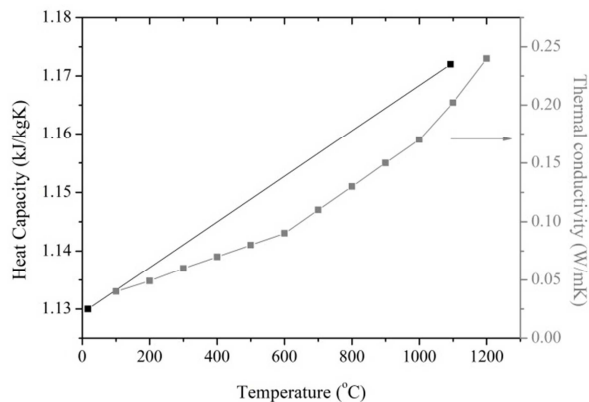


Fig. 2. Simulation setup for test case BC30W30H30 (left) and FR30W30H30 (right).

In the general context of compartment fire simulations, the quality of the utilized grid resolution is commonly assessed using the non-dimensional  $D^*/\delta x$  ratio, where  $D^*$  is a characteristic fire diameter and  $\delta x$  corresponds to the nominal size of the grid cell. The  $D^*/\delta x$  ratio corresponds to the number of computational cells spanning  $D^*$  and is representative of the adequacy of the grid resolution. If the value of the  $D^*/\delta x$  ratio is sufficiently large, the fire can be considered well resolved. Several studies have shown that values of 10 or more are required to adequately resolve most fires and obtain reliable flame temperatures [5, 13]. In the current study, aiming to fulfil the  $D^*/\delta x \geq 10$  criterion and, at the same time, reduce the required computational cost, a 0.02 m cell size was selected ( $D^*/\delta x = 10$ ). The numerical grid extends to the outside of the enclosure, in order to effectively simulate air entrainment phenomena through the opening and burning outside the compartment. The size of the physical domain “extensions”, 1.0 m in the x- and 1.5 m in the z-direction, have been selected following findings in a relevant study on the effect of computational

domain size on numerical simulation of compartment fire [14]. The outer dimensions of the simulation domain are depicted in Fig. 2 and the computational grid consists of 375,000 cubic cells.

The measured heat release rate was used as an input to the FDS simulations. All walls, including the façade wall, consist of fiberboard with the following properties: 0.02 m thickness, 300 kg/m<sup>3</sup> density, 0.9 emissivity, thermal conductivity and heat capacity temperature-dependent values according to the manufacturer as depicted in Fig. 3. The soot yield, which represents the fraction of ethanol fuel mass converted to smoke particulates, is set equal to 0.8% and the corresponding CO yield was set equal to 0.1%, according to available measurements for ethanol [12]. The entire computational domain (both indoors and outdoors) is assumed to be initially still (zero velocity), exhibiting a temperature of 20°C. Concerning turbulence modelling, both turbulent  $Sc$  and  $Pr$  values were chosen to be equal to 0.5. There is no rigorous justification for these choices other than through direct comparison with experimental data for strong buoyant flows originating from enclosure fires occurring inside compartments [6]. For the radiative transport equation, 104 control angles are used, whereas time and angle increments are valued 3 and 5 respectively. Concerning the radiation solver, it is assumed that the gas behaves as a grey medium with a 0.125 m path-length  $L$  for RADCAL calculations. The total simulation time is selected to be equal to the respective duration of each test case, c.f. Table 1. Open boundaries are imposed at all boundaries external to the enclosure and wall boundary conditions are used at walls, ceiling and floor. Numerical results of the temporal evolution of gas temperatures, flame heights and heat fluxes for the interior and the exterior of the configuration were compared to available experimental data [1].



**Fig. 3.** Temperature-dependent values of heat capacity and thermal conductivity for the fibreboards used in the compartment's walls.

### Effect of pan position

To that respect, Figs. 4 and 5 present the spatial distribution of the instantaneous gas temperature inside the corridor for two characteristic test cases where the burner is located at the back and front of the corridor, respectively. During *Region I*, corresponding to 120 s from fire initiation, low gas temperatures are observed in the lower layer as fresh air enters the enclosure through the opening, located at the far right side of the corridor. In both cases, FDS accurately predicts the spatial distribution and the entrainment of fresh air into the corridor. In test case BC30W30H30, during *Region II*, where 400 s was chosen as an indicative time instance, the highest temperatures are observed in the vicinity of Boxes E and D indicating that combustion mainly takes place at these locations and flames gradually propagate towards the opening seeking available oxygen [15, 16]. FDS results, though able to depict the gas temperature vertical stratification, do not accurately reproduce the combustion zone; for instance, in the numerical simulation of the BC30H30W30 test case the fire plume is mainly located at the back of the corridor, at Box F, near the vicinity of the burner. This results in higher temperatures developed and stronger recirculation zone formed.

During *Region III*, the difference of gas temperatures between the upper and lower layers decreases towards the closed end (far left) of the corridor, but still, they cannot be assumed uniform inside the corridor. In *Region III*, at 900 s, flames fill the upper layer of the corridor extending towards the opening and eventually emerge from the opening when the HRR becomes sufficiently large. FDS captures well the phenomenon that the flame detaches from the burner after external burning was observed as depicted in the FDS spatial temperature distribution, though higher temperature levels can be observed. In test case FR30W30H30, temperature stratification in the interior of the corridor is less evident, since EVF emerge more quickly from the opening resulting in lower temperatures in Boxes C to F. Overall, predictions of gas temperature in the interior of the corridor show good levels of qualitative agreement with measured values; FDS accurately predicts the presence of the fire plume in the vicinity of Box A, resulting in the emergence of EVF outside the corridor.

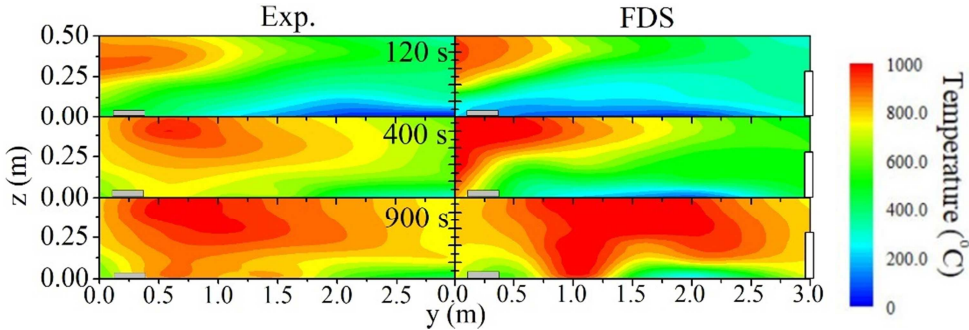


**Fig. 4.** Spatial distribution of the gaseous temperature at the corridor interior (BC30W30H30).

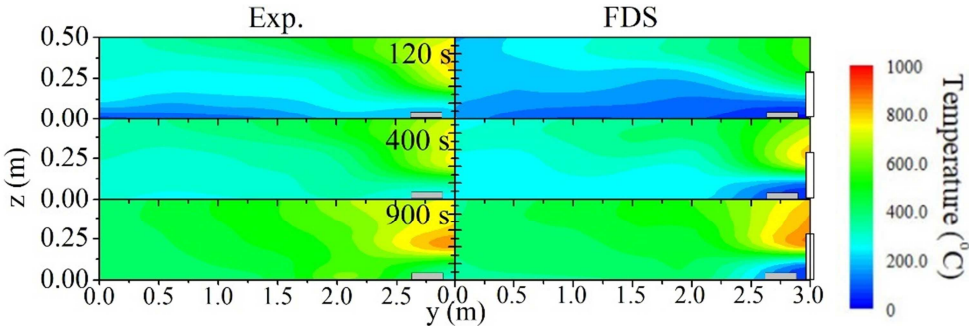


**Fig. 5.** Spatial distribution of the gaseous temperature at the corridor interior (FR30W30H30).

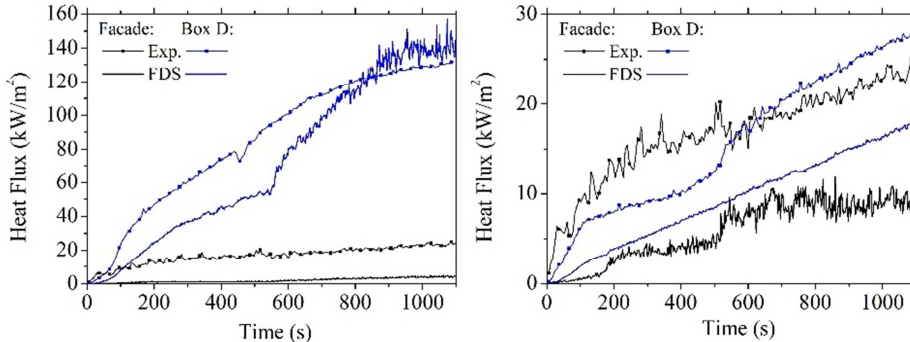


**Fig. 6.** Predictions and measurements of the temporal evolution heat fluxes for test cases BC30W30H30 (left) and FR30W30H30 (right).

The temporal evolution of the heat fluxes at the floor level of Box D and on the façade centreline at 38 cm above the ground, are illustrated in Fig. 6. In the BC30W30H30 test case, most of the combustion occurs inside the corridor, resulting in much higher heat fluxes on the corridor floor. Though FDS accurately predicts the heat flux evolution at the ground floor of the corridor, especially during *Region III*, it considerably underpredicts the heat flux on the façade centreline due to the underprediction of the external burning. In the FR30W30H30 test case, where the fuel pan is located close to the opening and EVF almost instantly eject through the opening, exposing the façade to significantly increased heat flux values, FDS qualitatively indicates the EVF emergence and subsequent façade heat exposure.

## EFFECT OF VENTILATION FACTOR

Figure 7 illustrates the temporal evolution of the measured and predicted upper layer gas temperatures at a height of 48 cm in Boxes A, C and E for all test cases. In order to quantify the predictive capability of the numerical model and to facilitate comparison between those time-dependent quantities, the metrics  $\varepsilon_1$  and  $\varepsilon_2$ , as defined and used for fire simulations by Audouin et al. [17] and the ASTM E1355-97 [18] standard guide, are calculated according to Eq. (1), where  $x$  and  $y$  represent experimental and numerical values. Results of the respective functional analysis used to compare the time-dependent values for the upper layer temperatures for Boxes A and E are presented in Table 2. The lowest values for the projection coefficient  $\varepsilon_1$  and respectively the highest for the inner product cosine  $\varepsilon_2$  are highlighted respectively to assist the interpretation of the results.

$$\varepsilon_1 = \frac{\|\bar{y} - \bar{x}\|}{\|\bar{x}\|} = \sqrt{\frac{\sum_{i=1}^n (y_i - x_i)^2}{\sum_{i=1}^n (x_i)^2}}, \quad \varepsilon_2 = \cos(\bar{x}, \bar{y}) = \frac{\langle \bar{x}, \bar{y} \rangle}{\|\bar{x}\| \|\bar{y}\|} = \frac{\sum_{i=1}^n x_i y_i}{\sqrt{\sum_{i=1}^n (x_i)^2} \sqrt{\sum_{i=1}^n (y_i)^2}} \quad (1)$$

Generally, predictions of the gas temperature in the interior of the corridor show good levels of qualitative agreement with measured values. In more details, it was found that gas temperatures in the interior of the corridor when the burner was located at the back of the corridor exhibited significantly higher temperatures, as is also depicted in the spatial temperature distribution presented in Fig. 4. In under-ventilated cases with low ventilation factors (e.g. BC30W25H25), FDS underpredicts the experimental values in the vicinity of the burner and the fire plume location is not accurately predicted. Higher ventilation factors result in more accurate predictions both in the front and the rear of the corridor and trends are accurately captured. EVF are predicted to eject through the opening consistently but temperature profiles in *Region III* do not remain constant for test cases BC30W30H30, BC30W50H25 and FR30W50H25. In FDS simulations, the flame plume moves towards the opening more intensively compared to the experiments, thus resulting in underprediction of temperatures at the back of the corridor and overprediction in the vicinity of the opening at Box A. When the burner was positioned near the opening in over-ventilated cases (e.g. FR30W25H25 and FR30W50H50), gas temperatures in the interior are substantially underpredicted, c.f. Table 2.

Numerical simulation results are further used to provide additional information regarding the flow field developed in the interior of the corridor and the exterior in the vicinity of the façade. Predictions of the gas phase velocity along with the resulting fire plume and resulting EVF envelope at 900 s after fire initiation in *Region III*, are depicted in Fig. 8. In FDS there is a limit on the amount of volumetric HRR released in each grid cell. By default, an empirical value of  $200 \text{ kW/m}^3$  is used as a limit based on the grid size which is also used in the current analysis of the numerical simulations. The effect of burner position on the predicted fire plume shape and velocity field is evident. In under-ventilated test cases, FR30W30H30, FR30W50H25 and BC30W25H25,

BC30W50H25, BC30W50H50, a significant portion of combustion takes place outside the corridor. This is due to the inadequate mass air flow rate that cannot sustain complete combustion, thus resulting in unburnt gaseous fuel and smoke exiting the corridor which leads to a more intensified EVF.

**Table 2. Errors  $\epsilon_1$  and  $\epsilon_2$  for Boxes A and E for all simulated test cases**

| Test cases | Box A        |              | Box E        |              |
|------------|--------------|--------------|--------------|--------------|
|            | $\epsilon_1$ | $\epsilon_2$ | $\epsilon_1$ | $\epsilon_2$ |
| FR30W25H25 | 0.47         | 0.988        | 0.35         | 0.995        |
| FR30W30H30 | <b>0.12</b>  | <b>0.992</b> | 0.44         | <b>0.998</b> |
| FR30W50H25 | 0.33         | 0.971        | 0.20         | 0.992        |
| FR30W50H50 | 0.24         | 0.957        | <b>0.08</b>  | 0.965        |
| BC30W25H25 | 0.33         | 0.998        | <b>0.32</b>  | 0.992        |
| BC30W30H30 | 0.42         | 0.936        | 0.78         | 0.937        |
| BC30W50H25 | <b>0.22</b>  | 0.998        | 0.82         | 0.987        |
| BC30W50H50 | 0.26         | <b>0.999</b> | 0.97         | <b>0.995</b> |

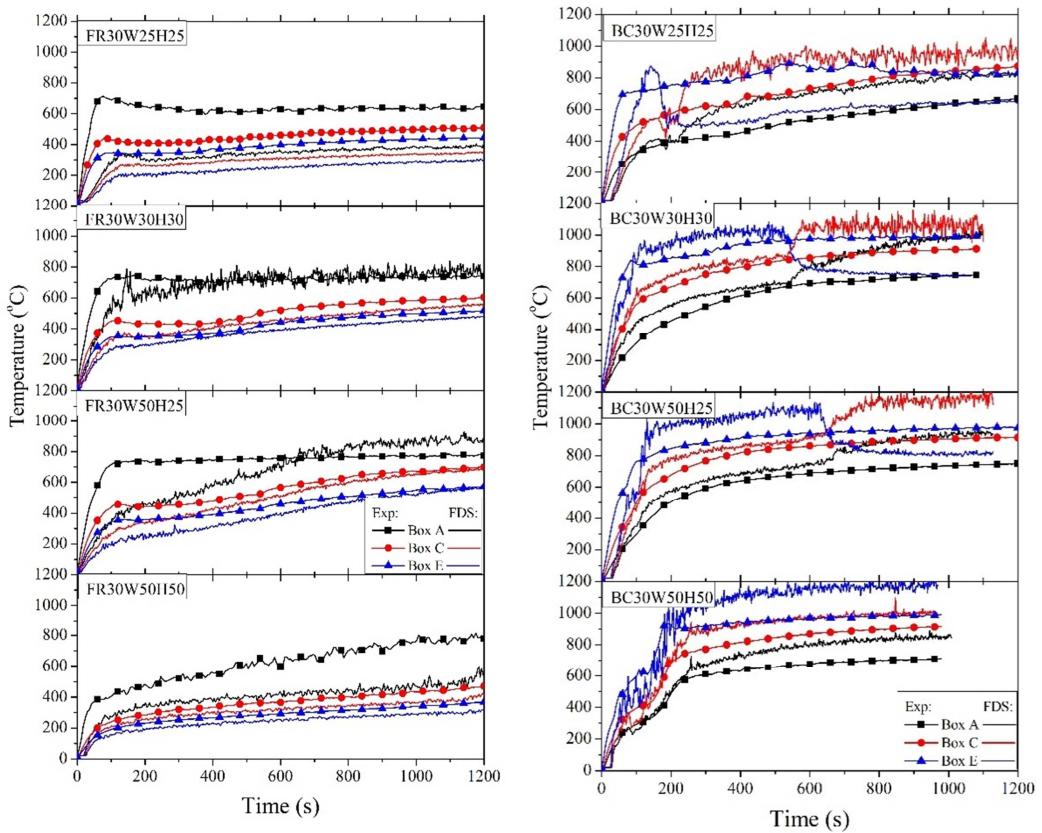


**Fig. 7.** Experimental and numerical temporal evolution of the gas temperature at a height of 45 cm in the interior of the corridor in Boxes A, E and E for FR (left) and BC (right) test cases.

Figure 9 depicts the vertical distribution of the time-averaged (over *Region III*) radiative heat flux measured using thin steel plate probes [16, 19] at the centreline of the façade for all test cases. Measured heat fluxes decrease with increasing height, as expected. The highest heat flux is located always along the centreline, except for test cases when the front of the enclosure is completely open, i.e., BC30W50H50 and FR30W50H50. Measured heat flux values are generally higher than predictions in all test cases and predictions in decreased ventilation areas indicate better agreement with experimental data. Nevertheless, the discrepancies are larger for cases where the burner is positioned at the rear of the corridor and cases where the width of the opening equals that of the corridor. Those cases include the fuel-controlled cases, where the predictive ability of FDS is known to be lacking.

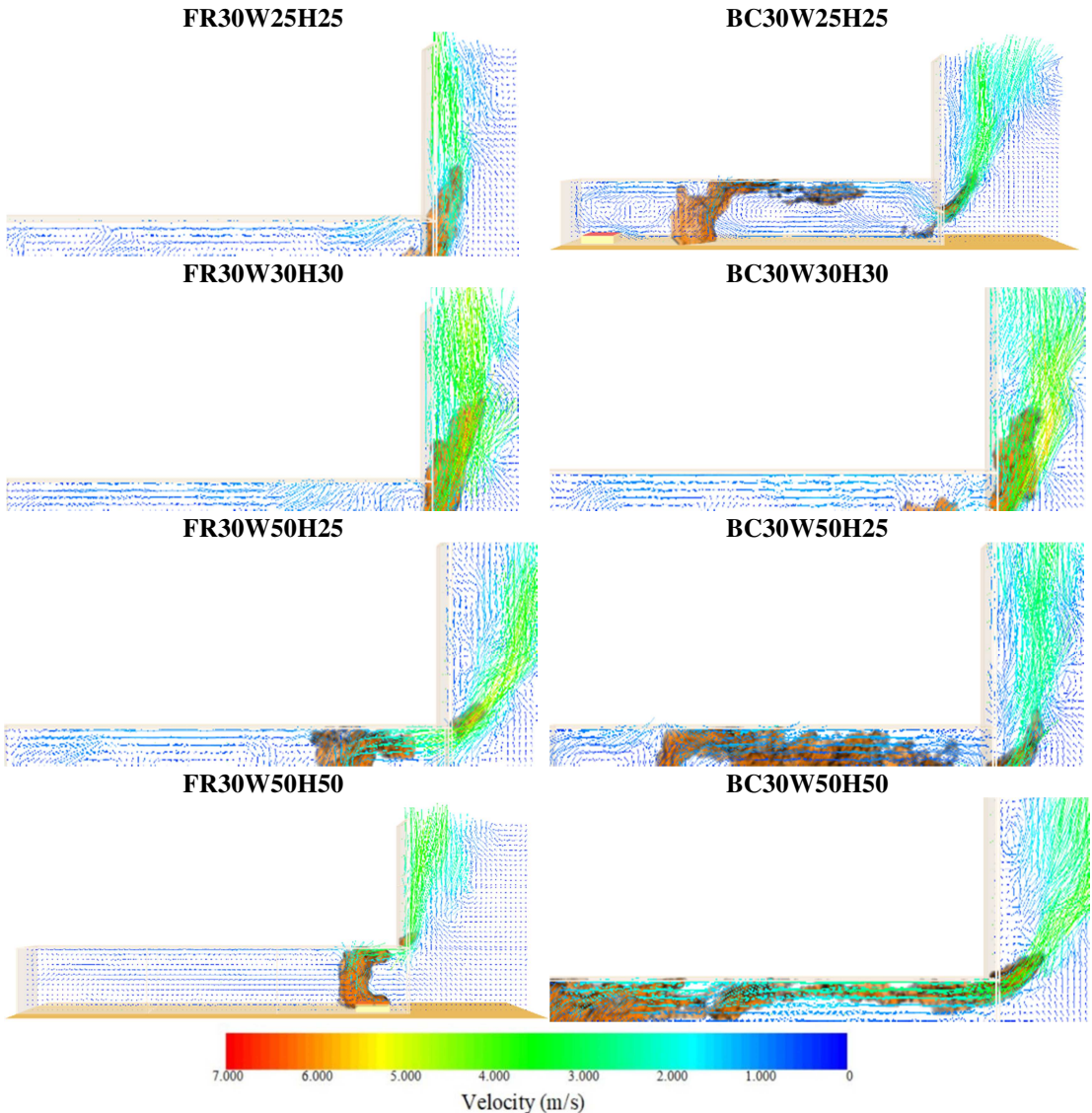


**Fig. 8.** Predictions of velocity vectors and flame envelope 900 s after fire initiation, corresponding to *Region III*, for all test cases.

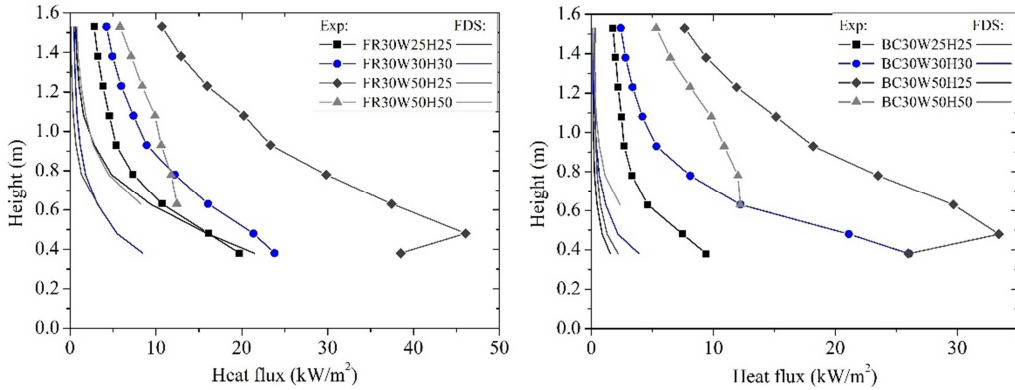


**Fig. 9.** Vertical distribution of time-averaged heat flux at the centerline of the façade for the FR (left) and BC (right) test cases.

## CONCLUSIONS

The dynamic nature of EVF requires the use of advanced modelling methodologies, capable of describing the relevant physical phenomena in sufficient detail. The commonly used prescriptive methodologies are based on a phenomenological approach that exhibits certain limitations, especially when unusual structures are considered. CFD tools may provide significant assistance to the fire safety engineering analysis of EVF, by offering the opportunity to obtain an in-depth view of the spatial and temporal distribution of important physical parameters such as velocity, gas temperatures, wall temperatures, heat fluxes, etc. In the current work, an extended series of medium-scale fire tests using liquid pool fires was analysed numerically, aiming to investigate the effect of pan location and ventilation parameters. The obtained predictions are compared to available experimental data. The main conclusions of this work can be summarized as follows:

1. In the interior of the corridor, good qualitative and occasionally quantitative agreement is observed for the gas temperatures. FDS captures well the detachment and propagation of the flame when the burner is positioned at the back of the corridor. However, FDS generally underpredicts the combustion zone and the fire plume seems tilting at the rear of the corridor.
2. The performance of the CFD tool in predicting EVF gas temperatures and heat flux to the adjacent façade is improved for larger opening sizes. Regarding the heat flux at the exposed surface of the façade, good quantitative agreement is observed, especially at lower heights near the opening. However, FDS generally underpredicts experimental values under over-ventilated conditions.
3. The present work provides a framework towards understanding the physics of the fire growth in corridor-shaped structures, but future experiments should aim at further investigating the effect of corridor geometry (e.g. investigation of different aspect ratios and geometrical configurations). The predictive ability of the numerical model will be further assessed by using a larger dataset of medium- and full-scale corridor-façade fire configurations in a range of realistic fire scenarios.

## ACKNOWLEDGEMENTS

The present work has been financially supported by “ELISSA: Energy Efficient Lightweight-Sustainable-Safe-Steel Construction” project (FP7-2013-NMP-ENV-EeB). Technical assistance of Mr. M. McKee, Mr. B. Veighy and Mr. K. Kowalski is gratefully acknowledged.

## REFERENCES

- [1] K. Chotzoglou, E. Asimakopoulou, J. Zhang, M.A. Delichatsios, Experimental investigation of liquid pool fires and externally venting flames in corridor-like enclosures, In: Conference Proceedings of the 10th International Conference on Structures in Fire 2018, pp, 901-909, 2018.
- [2] K. Chotzoglou, E. Asimakopoulou, J. Zhang, M.A. Delichatsios, An experimental investigation of burning behaviour of liquid pool fire in corridor-like enclosures, In: Conference Proceedings of the European Symposium on Fire Safety Science, 2018.
- [3] K. Chotzoglou, E. Asimakopoulou, J. Zhang, M.A. Delichatsios, Experimental investigation of externally venting flames geometric characteristics and impact on the façade of corridor-like enclosures, In: Conference Proceedings of the European Symposium on Fire Safety Science, 2018.
- [4] E. Yii, C. Fleischmann, A. Buchanan, Vent flows in fire compartments with large openings, *J. Fire Prot. Eng.* 17 (2007) 221-237.
- [5] C.Y. Lin, Study of exposure fire spread between buildings by radiation, *J. Chinese Inst. Eng.* 23 (2000) 493-504.
- [6] D. Yang, L.H. Hu, Y.Q. Jiang, R. Huo, S. Zhu, X.Y. Zhao, Comparison of FDS predictions by different combustion models with measured data for enclosure fires, *Fire Safety J.* 45 (2010) 298-313.
- [7] W. Zhang, A. Hamer, M. Klassen, D. Carpenter, R. Roby, Turbulence statistics in a fire room model by large eddy simulation, *Fire Safety J.* 37 (2002) 721-752, 2002.
- [8] J.E. Floyd, Comparison of CFAST and FDS for fire simulation with HDR T51 and T52 tests, National Institute of Standards and Technology, NISTIR 6866, U.S., 2002.
- [9] S. Yuan S., J. Zhang, Large eddy simulation of compartment fire with solid combustibles, *Fire Saf. J.* 44 (2009) 349-632, 2009.
- [10] H.Y. Wang, Numerical study of under-ventilated fire in medium-scale enclosure, *Build. Environ.* 44 (2009) 1215-1227.
- [11] C.A. Empis, Analysis of the compartment fire parameters influencing the heat flux incident on the structural façade, Ph.D. Thesis, University of Edinburgh, U.K., 2010.
- [12] M.J. Hurley, Performance-Based Design, SFPE handbook of fire protection engineering, SFPE, 1233-1261, 2016.
- [13] D.I. Kolaitis, E.K. Asimakopoulou, M.A. Founti, Fire behaviour of gypsum plasterboard wall assemblies: CFD simulation of a full-scale residential building, *Case Studies in Fire Safety* 7 (2017) 23-35.
- [14] X. Zhang, M. Yang, J. Wang, Y. He, Effects of computational domain on numerical simulation of building fires, *J. Fire Prot. Eng.* 20 (2010) 225-250.
- [15] Y.P. Lee., M.A. Delichatsios, G. Silcock, Heat fluxes and flame heights in façades from fires in enclosures of varying geometry, *Proc. Comb. Inst.* 31 (2007) 2521-2528.
- [16] J. Zhang, M.A. Delichatsios, Determination of the convective heat transfer coefficient in three-dimensional inverse heat conduction problems, *Fire Saf. J.* 44 (2009) 681-690.
- [17] L. Audouin, L. Chandra, J.L. Consalvi, L. Gay, E. Gorza, V. Hohm, S. Hostikka, T. Ito, W. Klein-Hessling, C. Lallemand, T. Magnusson, N. Noterman, J.S. Park, J. Peco, L. Rigollet., S. Suard, P. Van-Hees, Quantifying differences between computational results and measurements in the case of large scale well confined fire scenario, *Nucl. Eng. Design* 241 (2011) 18-31.
- [18] ASTM E1355-97, Standard guide for evaluating the predictive capability of deterministic fire models, American Society for Testing and Materials International, West Conshohocken, U.S., 2006.
- [19] Y. Lee, M.A. Delichatsios, G.W.H. Silcock, Heat flux distribution and flame shapes on the inert façade, *Fire Saf. Sci.* 9 (2008) 193-204.